Cell fusion in yeast is negatively regulated by components of the cell wall integrity pathway

Allison E. Hall[a,†] and Mark D. Rose[a,b,*]
[a]Department of Molecular Biology, Princeton University, Princeton, NJ 08544; [b]Department of Biology, Georgetown University, Washington, DC 20057

ABSTRACT During mating, *Saccharomyces cerevisiae* cells must degrade the intervening cell wall to allow fusion of the partners. Because improper timing or location of cell wall degradation would cause lysis, the initiation of cell fusion must be highly regulated. Here, we find that yeast cell fusion is negatively regulated by components of the cell wall integrity (CWI) pathway. Loss of the cell wall sensor, *MID2,* specifically causes "mating-induced death" after pheromone exposure. Mating-induced death is suppressed by mutations in cell fusion genes (*FUS1, FUS2, RVS161, CDC42*), implying that *mid2Δ* cells die from premature fusion without a partner. Consistent with premature fusion, *mid2Δ* shmoos had thinner cell walls and lysed at the shmoo tip. Normally, Cdc42p colocalizes with Fus2p to form a focus only when mating cells are in contact (prezygotes) and colocalization is required for cell fusion. However, Cdc42p was aberrantly colocalized with Fus2p to form a focus in *mid2Δ* shmoos. A hyperactive allele of the CWI kinase Pkc1p (*PKC1**) caused decreased cell fusion and Cdc42p localization in prezygotes. In shmoos, *PKC1** increased Cdc42p localization; however, it was not colocalized with Fus2p or associated with cell death. We conclude that Mid2p and Pkc1p negatively regulate cell fusion via Cdc42p and Fus2p.

INTRODUCTION

Cell fusion is an essential process in eukaryotic organisms. In mammals, in addition to fertilization, fusion occurs during a variety of developmental processes, including placental trophoblast fusion during pregnancy, osteoclast formation, and the fusion of myoblasts to form myofibers during skeletal muscle development (Abmayr *et al.*, 2008; Abmayr and Pavlath, 2012; Alper and Podbilewicz, 2008; Huppertz and Borges, 2008; Ishii and Saeki, 2008; Jansen and Pavlath, 2008; Wassarman and Litscher, 2008; Mugnier *et al.*, 2009). Inhibition of cell fusion is detrimental; for example, blockage of placental trophoblast fusion has been linked to preeclampsia during pregnancy (Gauster *et al.*, 2009) and a defect in myoblast fusion

causes a congenital myopathy (Di Gioia *et al.*, 2017). Cell fusion must be temporally and spatially controlled so that cells fuse with the right partner and in the correct location.

During mating in *Saccharomyces cerevisiae*, two haploid cells fuse to form a diploid zygote (Madhani, 2007). Mating types **a** and α secrete specific pheromones that are detected by the opposite mating type. The cells polarize their growth along the pheromone gradient forming polarized cells called "shmoos." During shmooing, cells prepare for fusion, clustering vesicles near the zone of cell fusion that are thought to contain the hydrolases required for cell wall degradation (Baba *et al.*, 1989; Gammie *et al.*, 1998). When the mating cells come into contact with each other, continued growth and cell wall remodeling leads to a flat interface between the mating partners, a region called the zone of cell fusion (ZCF). During cell fusion, the cell wall is degraded starting at the center of the ZCF, allowing the plasma membranes to come into close contact. Plasma membrane fusion allows a continuous cytoplasm through which the two nuclei move together and eventually fuse (Gammie *et al.*, 1998; Ydenberg and Rose, 2008; Merlini *et al.*, 2013). Because aberrant cell wall degradation in this single-celled organism would lead to lysis and death, the correct timing and location of cell wall degradation is essential for the survival of *S. cerevisiae*.

Several key regulators of cell fusion have been described. Fus2p and Rvs161p form a heterodimeric amphiphysin that is transported

to the shmoo tip, where it is retained by Fus1p, Kel1p, and actin (Stein et al., 2015; Smith and Rose, 2016). Mutations affecting Fus1p, Fus2p, Kel1p, and Rvs161p cause failure of cell wall removal at the ZCF (Trueheart et al., 1987; Trueheart and Fink, 1989; Gammie et al., 1998; Smith and Rose, 2016). In wild-type (WT) mating pairs, after cell contact but before fusion, vesicles are observed to cluster adjacent to the ZCF (Gammie et al., 1998). Rvs161p and Fus2p are not required to localize the vesicles. In fus1 mutant prezygotes, the vesicles fail to localize, suggesting that Fus1p functions upstream of Rvs161p/Fus2p in the pathway (Trueheart et al., 1987; Gammie et al., 1998; Paterson et al., 2008). Activated Cdc42p binds to Fus2p (Ydenberg et al., 2012), and the Cdc42p/Fus2p/Rvs161p complex is postulated to catalyze exocytosis to release hydrolases into the ZCF to break down the cell wall (Gammie et al., 1998; Paterson et al., 2008). Cdc42p is a highly conserved Rho-GTPase that is involved in several steps in mating and cell fusion (Madden and Snyder, 1998; Johnson, 1999; Richman et al., 1999; Kozminski et al., 2000; Adamo et al., 2001; Perez and Rincon, 2010). In addition to signaling, Cdc42p plays a role in polarity establishment, actin cytoskeleton rearrangement, and secretion (Simon et al., 1995; Zhao et al., 1995; Nern and Arkowitz, 1998, 1999; Barale et al., 2006; Ydenberg et al., 2012). It has recently been shown that Cdc42p forms a discrete focus at the center of the ZCF during mating, dependent on Fus2p, Rvs161p, Fus1p, and Kel1p (Smith et al., 2017).

During normal mitotic growth, cell wall damage is rapidly repaired through the actions of the cell wall integrity (CWI) pathway. The CWI pathway contains five plasma membrane–associated integral-membrane proteins (Wsc1p, Wsc2p, Wsc3p, Mid2p, and Mtl1p) each containing highly O-mannosylated domains that extend into the cell wall (Gray et al., 1997; Verna et al., 1997; Jacoby et al., 1998; Ketela et al., 1999; Rajavel et al., 1999; Philip and Levin, 2001). The transmembrane proteins are hypothesized to be mechanosensors; changes in the cell wall sensed by the extracellular domains are thought to be transduced across the plasma membrane to intracellular regulatory proteins (Dupres et al., 2009; Heinisch and Dufrene, 2010). The CWI pathway has been shown to respond to cell wall stress from growth, polarization, heat, and drugs (Gray et al., 1997; Verna et al., 1997; Jacoby et al., 1998; Reinoso-Martin et al., 2003; Bermejo et al., 2010). The master regulator of the CWI pathway is Rho1p, a Rho-GTPase related to Cdc42p, which when bound by GTP, activates the sole protein kinase C (Pkc1p) in S. cerevisiae. Rho1p also functions in cell wall deposition, through association with Fks1p, the β-1,3 glucan synthase, and has effects on actin cytoskeleton organization and polarized secretion (Drgonova et al., 1996; Mazur and Baginsky, 1996; Ozaki et al., 1996; Qadota et al., 1996). Pkc1p activates downstream components of the CWI pathway, which culminates in the transcriptional activation of genes involved in cell wall biogenesis and the cell cycle (Levin, 2005, 2011). Pkc1p localizes to sites of polarized growth, where cell wall remodeling is active (Heinisch and Rodicio, 2018). However, in response to localized cell wall damage, Pkc1p rapidly relocalizes to the site of damage (Levin et al., 1990; Nonaka et al., 1995; Kamada et al., 1996; Kono et al., 2012). Given a very active surveillance of CWI, how do cells allow cell wall degradation to occur at the ZCF during mating? We hypothesize that the CWI pathway must be locally down-regulated during cell fusion.

Consistent with this view, a dominant hyperactive PKC1 mutation (PKC1-R398P, referred to as a PKC1* in this article) causes a cell fusion defect (Philips and Herskowitz, 1997). One interpretation of this observation was that Pkc1p may negatively regulate cell fusion, and that the negative regulation must be overcome for cells to fuse

(Philips and Herskowitz, 1997). If Pkc1p regulates cell fusion, it is likely that upstream components of the CWI pathway do as well. Of the five transmembrane proteins in the CWI pathway, Wsc1p and Mid2p are the most important. In haploids, loss of WSC1 is sufficient to cause death by cell lysis at high temperatures. MID2 stands for "mating-induced death," because mid2Δ cells lose viability after exposure to mating pheromone (Errede et al., 1995; Buehrer and Errede, 1997; Gray et al., 1997; Verna et al., 1997; Ketela et al., 1999; Rajavel et al., 1999). However, the basis of mating-induced death has remained unclear. Suppression of mid2Δ by increased levels of calcium suggested that misregulated calcium signaling might be involved, as it is for the mid1 mutation affecting a calcium transporter (Iida et al., 1994). In mitotic cells, deletion of WSC1 and MID2 together causes cell death at normal temperatures, which can be suppressed by osmotic support (1M sorbitol; Ketela et al., 1999; Rajavel et al., 1999). Even WT cells undergo a degree of pheromone-induced death in the extended absence of mating partners, affecting up to 25% of cells (Zhang et al., 2006). Death occurs in two waves: a fast wave (~1.5 h after pheromone addition) and a slow wave (~9.5 h after pheromone addition). The CWI pathway, as well as Fus1p, Fus2p, and Rvs161p, play a role in the fast cell death, whereas calcium signaling via calcineurin is required for slow cell death (Zhang et al., 2006). Although the cause of fast cell death was not identified, it was suggested that it entailed increased levels of reactive oxygen species (Zhang et al., 2006).

Here we examine the role of Mid2p and Wsc1p in cell fusion. We show that the cause of mid2Δ death is unregulated cell fusion, leading to premature cell wall removal in shmoos before prezygote formation. Mid2p and Pkc1p regulate Cdc42p localization in shmoos and prezygotes. Our data suggest a role for Mid2p as a specific negative regulator of Fus2p in cell fusion, whereas Pkc1p regulates Cdc42p localization differently during polarization and fusion.

RESULTS

mid2Δ pheromone-induced death is due to loss of plasma membrane integrity

Cell wall degradation must be tightly regulated during mating to allow cells to properly fuse, while also preventing misplaced or premature fusion. A hyperactive allele of the sole protein kinase C in yeast, Pkc1p (PKC1-R398P, referred to as PKC1*), causes a cell fusion defect, suggesting that Pkc1p acts as a negative regulator of cell fusion (Philips and Herskowitz, 1997). Because Pkc1p is the central kinase in the CWI MAP kinase cascade (Levin et al., 1990; Nonaka et al., 1995), we hypothesized that the upstream transmembrane sensor proteins in the CWI pathway (Mid2p, Mtl1p, Wsc1p, Wsc2p, and Wsc3p), could serve as initial signals of this negative regulation of fusion. WSC1 and MID2 are sufficient to support mitotic growth; loss of both makes cells inviable in the absence of osmotic support (Supplemental Figure S1). We tested the effects on mating of deletion mutants in each of the genes; all five mutants exhibited WT levels of mating. However, mid2Δ mutants uniquely showed a mating-specific phenotype, pheromone-induced death in low calcium media, reaching ~70% inviability within 5 h (Rajavel et al., 1999; Philip and Levin, 2001). Although the pheromone sensitivity of mid2Δ was known previously (Ono et al., 1994; de Bettignies et al., 1999; Rajavel et al., 1999; Philip and Levin, 2001), the basis of mating-induced death remained unclear. The intact appearance of the cells, and the suppression of death by calcium or PKC1*, but not by osmotic support, suggested that death might be due to a downstream calcium signaling defect (Ketela et al., 1999). However, a specific target of calcium signaling has not been identified.
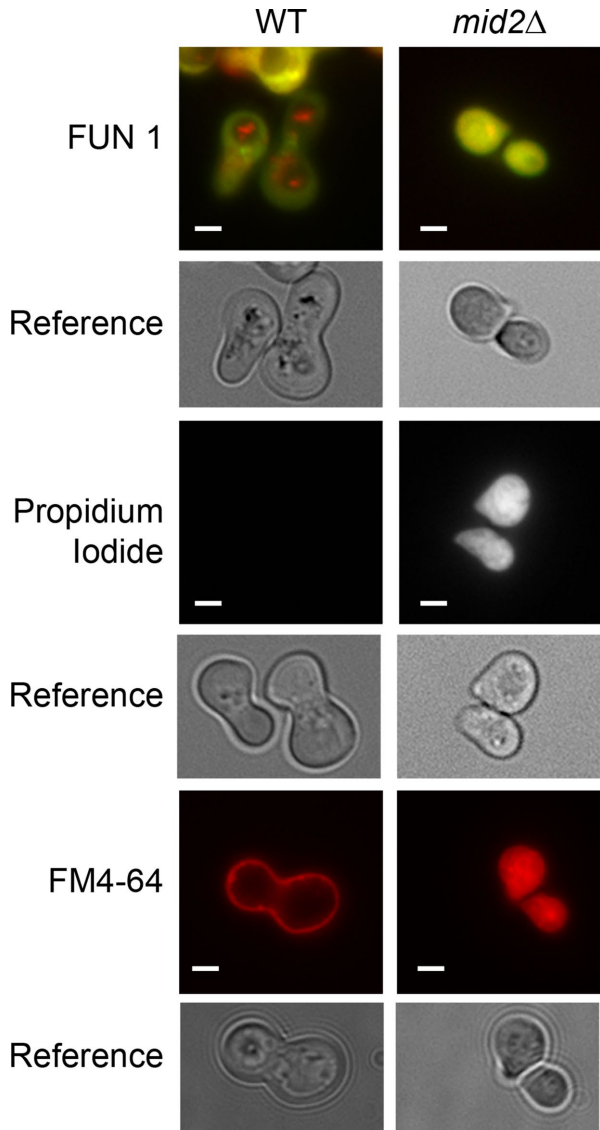
FIGURE 1: *mid2Δ* cells lose integrity upon pheromone exposure. WT (MY8092) and *mid2Δ* (MY14673) cells were treated with 8 μM α-factor for 5 h and Live/Dead stained (top panel), stained with propidium iodide (middle) or FM4-64 (bottom). For Live/Dead staining cells were treated with 15 μM FUN-1 and 25 μM Calcofluor White, incubated in the dark for 30 min and imaged; live (metabolically active) cells produce red fluorescence within the vacuoles, whereas dead cells stain bright yellow. Cells were stained with 20 μM propidium iodide for 15 min and imaged. Propidium iodide is excluded from living cells. FM4-64 stains the entirety of *mid2Δ* cells, but is restricted to the plasma membrane of WT cells. *n* > 100 cells. Scale bar = 2 μm.

To reexamine the nature of *mid2Δ* cell death, we used microscopy and a variety of vital dyes. Previous work utilized methylene blue staining (de Bettignies *et al.*, 1999), which has been suggested to be membrane permeable, but decolorized in living cells (Passow *et al.*, 1959). The fluorescent FUN 1 dye (Millard *et al.*, 1997) is also membrane permeable and stains the cytoplasm of all cells bright-green. In metabolically active cells, FUN 1 accumulates in the vacuole where it is converted into a red fluorescent molecule that forms distinctive aggregates. After exposure to pheromone, most WT cells exhibited weak green fluorescence in the cytoplasm and bright red aggregates in the vacuoles (Figure 1, top). In contrast, the *mid2Δ*

cells showed only bright-green cytoplasm, confirming that these cells are not metabolically active. Note that under these conditions, WT shmoos acquire an enlarged "peanut" shape, because they have been growing in pheromone for 5 h. In contrast, the *mid2Δ* cells abruptly stopped growing soon after the initial formation of the shmoo projection and are smaller and more pointed (Figure 1, top).

Because the FUN 1 dye readily crosses intact membranes, it does not report on the integrity of the plasma membrane. Propidium iodide is a membrane impermeant fluorescent dye that binds tightly to nucleic acids (Deere *et al.*, 1998). Live cells exclude the dye completely, but cells with damaged membranes stain brightly. As expected, the WT shmoos did not stain with propidium iodide (Figure 1, middle). In contrast, the *mid2Δ* shmoos showed intense diffuse staining, indicating that the plasma membrane was not intact. As a second way to probe the intactness of the plasma membrane, we used FM4-64, a membrane impermeant fluorescent dye that is often used to visualize vacuoles and endocytosis in live yeast (Fischer-Parton *et al.*, 2000; Yadav *et al.*, 2010). In intact cells, FM4-64 first stains the plasma membrane, but over time enters the cell by endocytosis and is transported to the vacuole membrane by vesicle trafficking. In WT shmoos, brief exposure to FM4-64 stained only the plasma membrane. In *mid2Δ* cells, addition of FM4-64 caused immediate bright staining of the entire cell cytoplasm (Figure 1, bottom). We conclude that the *mid2Δ* cells are losing viability due to loss of plasma membrane integrity, allowing rapid incorporation of FM4-64 and propidium iodide throughout the cell.

mid2Δ pheromone-induced death is due to premature cell fusion

Given that hyperactivation of the CWI pathway causes a block to cell fusion, we hypothesized that loss of an upstream positive regulator might cause pheromone-induced death due to aberrant or overactive fusion. To test this hypothesis, we deleted *FUS1* and *FUS2* or introduced cell fusion-specific alleles of *RVS161* and *CDC42* into the *mid2Δ* background. Cell death in pheromone was then measured using FM4-64 staining. Mutations in all four cell fusion proteins completely suppressed the *mid2Δ* pheromone-induced death (Figure 2A). Suppression was specific to genes affecting cell fusion; deletion of *KAR5*, required for nuclear fusion, had no effect. Fus2p and Rvs161p promote cell wall degradation in prezygotes, suggesting that *mid2Δ* pheromone sensitivity in shmoos is due to the premature activation of the cell fusion pathway, in the absence of a mating partner.

Given that loss of Mid2p may allow premature fusion, and that hyperactivation of Pkc1p blocks fusion, we reasoned that the CWI pathway might generally suppress cell wall removal in prezygotes. If so, then loss of the CWI sensors should partially compensate for the loss of cell fusion pathways during mating. Fus1p and Fus2p act in partially overlapping pathways to promote cell fusion (Trueheart and Fink, 1989; Gammie *et al.*, 1998; Ydenberg *et al.*, 2012). Deletion of either *FUS1* or *FUS2* causes a partial cell fusion block, with a cell wall remaining between the two mating partners (Gammie *et al.*, 1998). Deletion of either *MID2* or *WSC1* in both mating partners partially suppressed the fusion defects in *fus1Δ* × *fus1Δ* and *fus2Δ* × *fus2Δ* matings (Figure 2B) and the effects of *mid2Δ* and *wsc1Δ* are additive (Supplemental Figure S2A). Interestingly, suppression occurred under conditions where the downstream CWI protein kinase, Slt2p, did not appear to be active, suggesting that suppression is related to signaling from upstream components of the pathway (Supplemental Figure S2B). However, when cells lacked both *FUS1* and *FUS2*, fusion was completely blocked, and deletion of *MID2* or *WSC1* was not able to suppress the fusion defect (Figure 2B). These results suggest that the CWI pathway antagonizes cell wall removal;
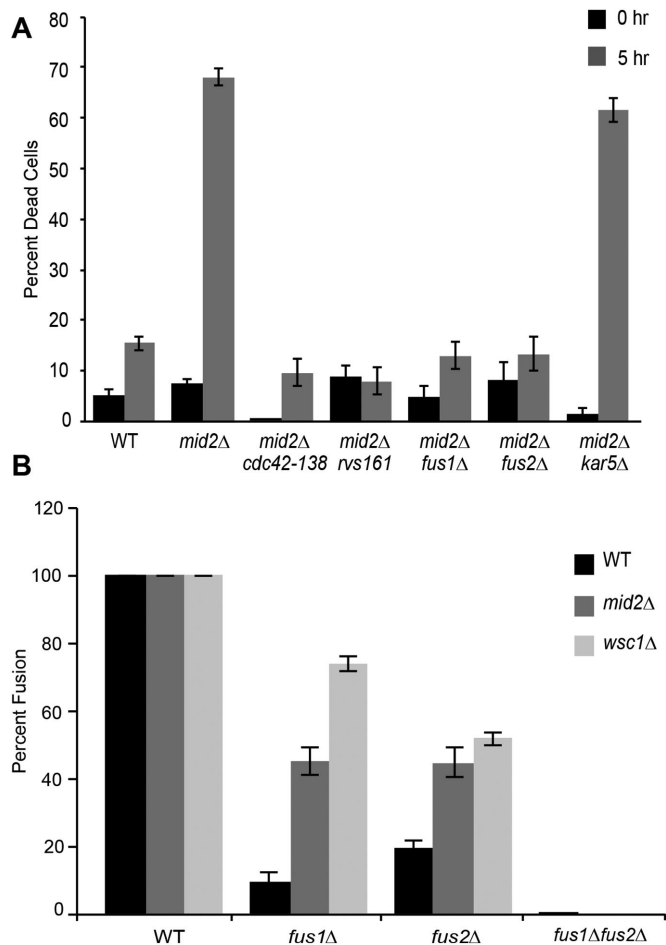
FIGURE 2: Components of the CWI pathway negatively regulate cell fusion. (A) *mid2Δ* death is suppressed by loss of cell fusion proteins. WT (MY8092), *mid2Δ* (MY14673), *mid2Δ cdc42-138* (MY15390), *mid2Δ rvs161* (MY15620), *mid2Δ fus1Δ* (MY15618), *mid2Δ fus2Δ* (MY15081), or *mid2Δ kar5Δ* (MY15628) were grown and exposed to pheromone as described in *Materials and Methods*, and dead cells were assessed using FM4-64 staining after 5 h in pheromone. (B) *MID2* and *WSC1* negatively regulate cell fusion. Each mating is bilateral, with the indicated deletion in both partners (WT with *mid2Δ* indicates *mid2Δ* x *mid2Δ* mating, *fus1Δ* with *wsc1Δ* indicates *fus1Δ wsc1Δ* × *fus1Δ wsc1Δ* mating). WT (8092 × 8093), *mid2Δ* (MY14673 × MY14674), *wsc1Δ* (MY14305 × MY14306), *fus1Δ* (JY427 × JY430), *fus2Δ* (MY9181 × MY9185), *fus1Δ fus2Δ* (MY10935 × JY429), *mid2Δ fus1Δ* (MY15618 × MY15619), *wsc1Δ fus1Δ* (MY15499 × MY15500), *mid2Δ fus2Δ* (MY15081 × MY15080), *wsc1Δ fus2Δ* (MY15072 × MY15073), *mid2Δ fus1Δ fus2Δ* (MY16000 × MY16002), *wsc1Δ fus1Δ fus2Δ* (MY15489 × MY15490) were grown in YEPD, mated for 3 h at 30°C, stained with FM4-64, and imaged. Fusion was counted as any cell that was fully fused or partially fused (some plasma membrane remaining between the mating partners). Error bars denote SEM. *n* > 100 cells, in three or more independent experiments.

however, loss of negative regulation cannot overcome complete loss of cell fusion–dependent cell wall removal. These observations support the premise that the pheromone sensitivity of *mid2Δ* is due to premature cell fusion.

mid2Δ cells lose CWI at their shmoo tip

FM4-64 staining showed that *mid2Δ* cells lose plasma membrane integrity, but did not test whether the cells also lose CWI, as would be expected from premature cell wall removal. The intact appear-

ance of *mid2Δ* shmoos by transmitted light microscopy suggested that any loss of CWI must be spatially restricted. To address this, we used live cell imaging of *mid2Δ* cells as they responded to pheromone. The cells contained cytoplasmic GFP to determine when they lost integrity. In typical videos, GFP was rapidly lost soon after the cells formed shmoo projections; beginning at the shmoo tip. In some images, cellular debris was observed being ejected from the shmoo tip, concomitant with loss of cytoplasmic GFP signal (Figure 3A). These observations strongly suggested that cell death was due to loss of cell integrity at the shmoo tip.

To determine where *mid2Δ* cells were suffering cell wall removal, we used transmission electron microscopy and found that *mid2Δ* cells have a thinner cell wall at the shmoo tip (Figure 3B). To correct for differences in the angle of the sections during quantification, we measured the thickness of the cell wall at both the shmoo tip and the base of the cell (opposite the shmoo tip) and determined the ratio (cell/shmoo tip) (Figure 3, B and C). In WT shmoos, the mean ratio was 1 ± 0.49, indicating that the cell wall is normally the same thickness at the shmoo tip as elsewhere. In contrast, *mid2Δ* cells had significantly thinner cell walls at the shmoo tip than WT cells (mean = 3.0 ± 2, *p* value = 5 × 10⁻⁶, Student's *t* test; Figure 3, B and C). In many cells the cell wall at the shmoo tip appeared to be completely removed (Figure 3B). The *fus2Δ* and *wsc1Δ* mutants were not significantly different from WT (0.9 ± 0.53 and 1.2 ± 0.69, *p* value = 0.25 and 0.12). Thus, Fus2p and Wsc1p do not have major effects on cell wall thickness in otherwise WT shmoos. In contrast, the dramatic thinning of the shmoo-tip cell wall in the *mid2Δ* mutant was completely suppressed by *fus2Δ*, restoring it to WT (ratio = 1.1 ± 0.55, *p* value = 0.16). We conclude that the cause of *mid2Δ* pheromone-induced death is unregulated/premature cell wall removal specifically at the shmoo tip.

Mid2p negatively regulates Cdc42p localization at the shmoo tip

There are two plausible explanations for *mid2Δ* death. First, in the absence of Mid2p, cells might not sense the cell wall stress associated with shmoo formation. Without an effective CWI response, cell wall deposition might not keep pace with ongoing cell wall removal at the shmoo tip, mediated in part by the cell fusion machinery. Alternatively, Mid2p and the CWI pathway may directly regulate the Fus2p-dependent cell fusion machinery.

In WT cells responding to pheromone, Cdc42p is uniformly distributed over the shmoo-tip cortex for its general role in polarity. In prezygotes, as cell wall removal begins, Cdc42p forms a bright focus at the center of the ZCF, colocalizing with, and dependent on, Fus2p (Smith *et al.*, 2017). Because *mid2Δ* appears to cause premature activation of cell wall removal, we examined Cdc42p localization in these cells. In contrast to WT shmoos, which showed relatively uniform distribution of Cdc42p over the cortex, Cdc42p formed a bright focus at the tip of *mid2Δ* shmoos (Figure 4A). To quantify localization, we normalized for variable levels of expression in each cell by measuring GFP intensity along a line tracing the shmoo-tip cortex; fluorescence intensity at each point is expressed as a ratio to the average intensity at the base of the shmoo tip (Smith *et al.*, 2017). Overall, GFP expression in whole cells was comparable in WT and *mid2Δ* cells (ratio of 0.9 *mid2Δ*/WT). Cdc42p localization in *mid2Δ* was significantly higher than WT (*p* value < 0.02; Figure 4, B and C). Cdc42p localization was also assessed in a second CWI pathway mutant, *wsc1Δ*. In contrast to *mid2Δ*, *wsc1Δ* caused somewhat decreased Cdc42p localization (*p* value < 0.02; Figure 4, A–C). Thus, *mid2Δ* specifically causes formation of a prezygote-like localization pattern for Cdc42p.
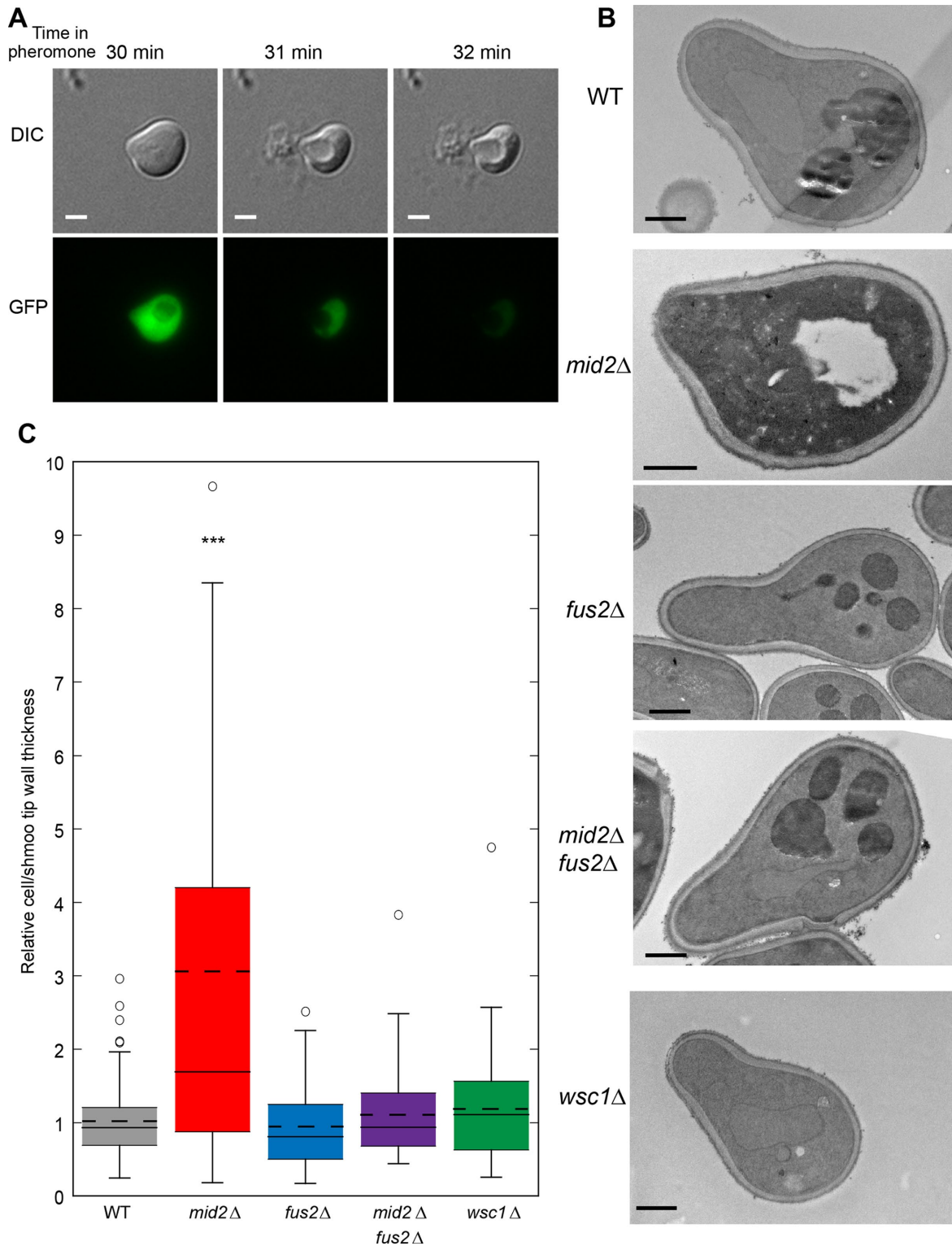
FIGURE 3: Loss of *MID2* causes cell wall degradation at the shmoo tip. (A) Representative image of *mid2Δ* cell lysing at the shmoo tip. *mid2Δ* cells (MY15807) with cytoplasmic GFP (Jin *et al.*, 2004) were grown to early log phase and plated on an agar pad made with low calcium media and 8 μM α-factor. Cells were imaged live over time, with images taken 1 min apart. Scale bar = 2 μm. (B) *mid2Δ* cells have thinner cell walls at the shmoo tip than other CWI or fusion pathway mutants. Box and whisker plot shows the ratio of cell wall thickness at the shmoo tip over the opposite side of the cell. Solid line indicates the median values, and dotted lines indicate mean values. WT (MY8092), *mid2Δ* (MY14673), *fus2Δ* (MY9181), *mid2Δfus2Δ* (MY15081), and *wsc1Δ* (MY14305) cells were exposed to 8 μM α-factor for 3 h and processed for EM imaging (see *Materials and Methods* for details). (C) Representative transmission electron microscopy images of the strains in B; sections are ~80 nm thick (see *Material and Methods* for details on fixing and staining). *n* > 68 cells for each strain. Scale bar = 800 nm.
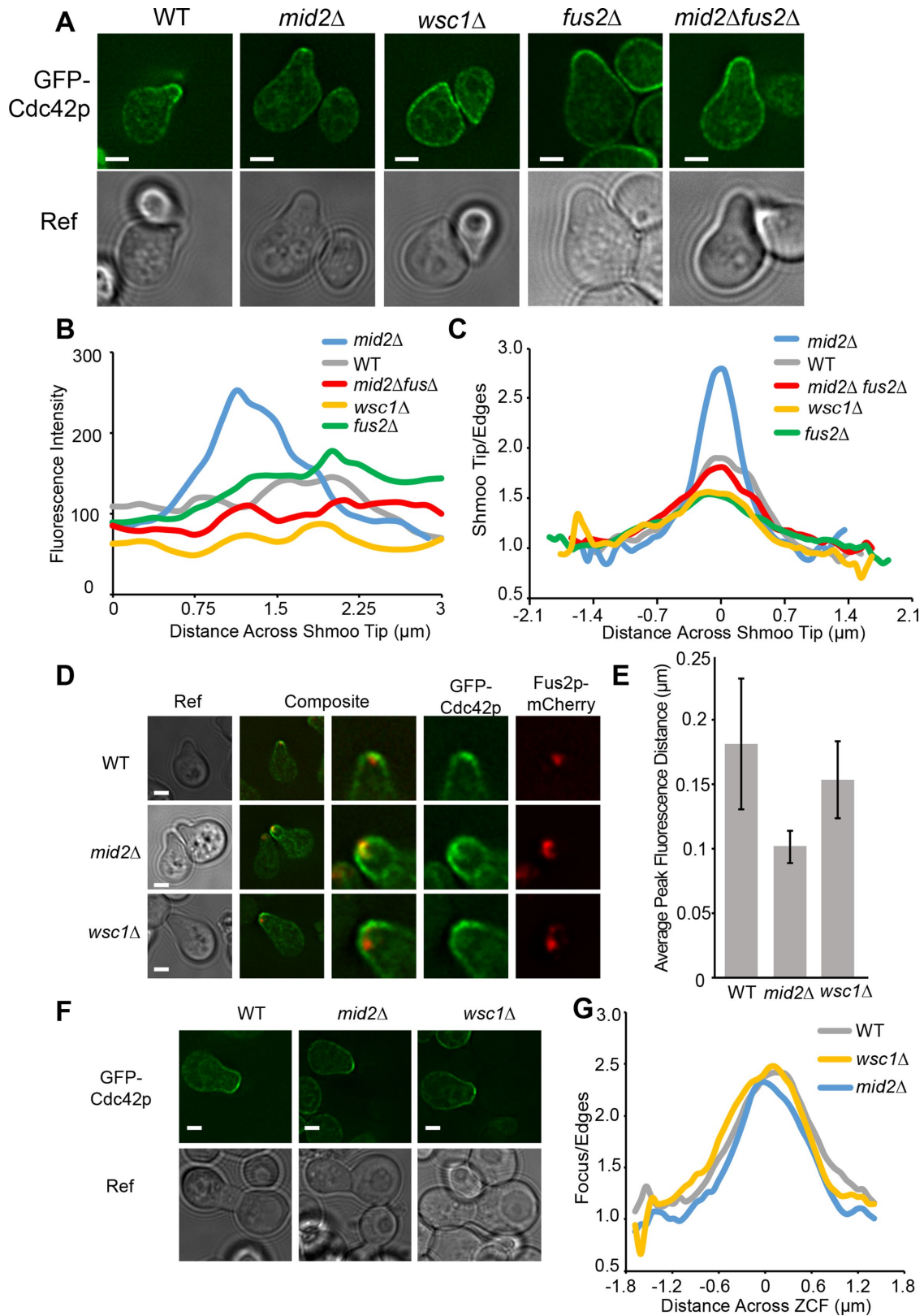
FIGURE 4: *MID2* negatively regulates Cdc42p localization. (A–C) Cdc42p forms a focus in *mid2Δ* shmoos, dependent on Fus2p. (A) Representative images of WT (MY15747), *mid2Δ* (MY15910) and *wsc1Δ* (MY15912), *fus2Δ* (MY15717), and *mid2Δfus2Δ* (MY16006) shmoos with GFP-Cdc42p (Dyer *et al.*, 2013) exposed to pheromone for 1.5 h, fixed with 2% formaldehyde for 10 min and imaged. (B, C) Quantification of GFP-Cdc42p fluorescence intensity in strains described in panel A. (B) Fluorescence intensity was measured along the shmoo-tip contour and plotted as a function of distance. Plots are for each of the individual cells in the representative images in panel A. (C) Combined fluorescence measurements for each of the indicated strains. Fluorescence intensity is expressed as the ratio of each point relative to

If Cdc42p localization in *mid2Δ* shmoos is a manifestation of premature cell fusion, then Cdc42p should colocalize with and be dependent on Fus2p. Formation of the Cdc42p focus at the shmoo tip in the *mid2Δ* mutant was completely blocked by *fus2Δ*, restoring localization to levels indistinguishable from WT (*p* value = 0.45; Figure 4, A–C). Therefore, Cdc42p shmoo-tip localization in a *mid2Δ* cell is Fus2p dependent. Interestingly, in *fus2Δ* shmoos, there was a small, but significant, decrease in Cdc42p shmoo-tip localization relative to WT (*p* value < 0.01), with a general increase in localization at more distal cortical regions (Figures 4, A–C and 5, F and G). Thus, a small fraction of the overall localization of Cdc42p at the shmoo tip is affected by Fus2p.

A hallmark of the Cdc42p focus at the ZCF is the precise colocalization with Fus2p (Smith *et al.*, 2017). In contrast, in WT shmoos Cdc42p and Fus2p are adjacent but not colocalized; in most cells (58%) there is no overlap between the proteins. This can be seen also by the average separation between the peaks of fluorescence intensity measured along an axis orthogonal to the cortex (Figure 4, D and E; Smith *et al.*, 2017). In the majority of *mid2Δ* shmoos (74%) Cdc42p and Fus2p were colocalized, with average peak intensities within ~0.1 μm (Figure 4, D and E). Colocalization was specific to *mid2Δ*; *wsc1Δ* shmoos were not significantly different from WT (Figure 4, D and E).

To determine whether these phenotypes carried over into prezygotes, we assessed Cdc42p localization during mating. We used *fus1Δ fus2Δ* partners to slow cell fusion and allow capture of this transient event (Smith *et al.*, 2017). In prezygotes, both *mid2Δ* (*p* value = 0.49) and *wsc1Δ* (*p* value = 0.62) showed a Cdc42p focus similar to WT, as expected from the lack of phenotypes in prezygotes (Figure 4, F and G). Moreover, *mid2Δ fus2Δ* prezygotes did not form a Cdc42p focus (Supplemental Figure S3). We infer that deletion of *MID2* and *WSC1* suppressed the fusion defects by limiting the cell's ability to rebuild the cell wall, rather than by increasing cell wall removal.

Deletion of downstream components of the CWI pathway, *SLT2* and *RLM1*, also shows some pheromone-induced death, 49 and 31% respectively, after 5 h in pheromone. However, unlike *mid2Δ*, *slt2Δ* pheromone-induced death is suppressed by the addition of osmotic support (1M sorbitol) to the media (Errede *et al.*, 1995). Suppression of *slt2Δ* by sorbitol suggests that death is due to reduced cell wall deposition during shmoo formation in the absence of an intact CWI pathway.

Pkc1p affects Cdc42p localization in shmoos and prezygotes
Hyperactive Pkc1p causes a moderate block to cell fusion (~20%; Philips and Herskowitz, 1997). Given the effect of *mid2Δ*, we reasoned that hyperactive *PKC1** might negatively affect Cdc42p localization in prezygotes. When a *PKC1** strain with GFP-Cdc42p was mated to a *fus1Δ fus2Δ* strain there was a significant decrease in Cdc42p at the ZCF compared with WT (*p* value = 0.047; Figure 5, A–C). We previously showed that curvature of the ZCF induced by

fps1Δ has a negative effect on Cdc42p localization in prezygotes (Smith *et al.*, 2017). Alone *fps1Δ* and *PKC1** cause 20–26% fusion failure; together the mutations cause cell fusion failure in 86% of zygotes (Philips and Herskowitz, 1997). This suggests that curvature and the CWI pathway play independent roles in regulating cell fusion.

Given that Cdc42p is recruited by Fus2p to form the focus at the ZCF (Smith *et al.*, 2017), we asked whether the effect was due solely to decreased recruitment by Fus2p. If so, then *fus2Δ* should be epistatic to *PKC1**, and the *fus2Δ PKC1** double mutant should be identical to *fus2Δ*. As previously reported, the *fus2Δ* prezygotes showed a large decrease in Cdc42p localization relative to WT (*p* value < 0.001). The *PKC1* fus2Δ* prezygotes showed a slight further decrease in Cdc42p localization relative to *fus2Δ* (Figure 5, A–C). These data suggest that the *PKC1**-mediated decrease in Cdc42p localization acts largely through regulation of recruitment by Fus2p. To confirm this finding, we examined their colocalization in prezygotes. In WT, the Cdc42p focus is precisely colocalized with Fus2p at the center of the ZCF (Figure 5, D and E), with peak fluorescence intensities separated by <0.06 μm, on average. In contrast, colocalization was perturbed in the *PKC1** prezygotes. Although both Fus2p and Cdc42p localized near the cortex, they were not strongly colocalized; the fluorescence intensity peaks were separated by almost 0.12 μm on average (Figure 5, D and E). Given that Fus2p was properly localized in the *PKC1** prezygotes, these observations suggest that Pkc1p may regulate Cdc42p localization by affecting the interaction with Fus2p.

We next examined the effect of *PKC1** in shmoos. Because *mid2Δ* and *PKC1** should have opposing effects on the CWI signaling pathway, we expected that Cdc42p would also show reduced localization in shmoos. Surprisingly, the *PKC1** mutant showed a bright Cdc42p focus at the shmoo tip, similar to *mid2Δ*, and significantly brighter than WT (*p* value = 0.01; Figure 5, F and G). However, because Cdc42p has multiple roles during shmoo formation, and because the *PKC1** shmoos do not lyse, we hypothesized that Cdc42p localization might reflect these alternate functions. If so, then increased localization of Cdc42p in *PKC1** shmoos should be at least partially independent of Fus2p. Introduction of *PKC1** into the *fus2Δ* mutant caused a significant increase in Cdc42p localization to the shmoo tip, relative to *fus2Δ* alone (*p* value < 0.001), although a focus did not form (Figure 5F). Taken together these data suggest that hyperactivation of Pkc1p increases localization of Cdc42p to the shmoo tip, in a manner that is mostly independent of Fus2p. However, when Fus2p is present, the combined effects cause formation of a Cdc42p focus.

It remained possible that Pkc1p positively regulates Fus2p localization (and/or Cdc42p interaction) in shmoos, unlike its negative role in prezygotes. To test this, we examined Fus2p and Cdc42p colocalization in *PKC1** shmoos. As previously reported, Cdc42p did not colocalize with Fus2p in WT shmoos (Figures 4, D and E, and 5, H and I; Smith *et al.*, 2017). In *PKC1** shmoos, Cdc42p also did not colocalize with Fus2p (Figure 5, H and I). These observations

the intensity measured at the edge of the contour. *n* > 80 shmoos for each strain. (D, E) Cdc42p and Fus2p colocalize in *mid2Δ* shmoos. WT (MY15747), *mid2Δ* (MY15910), and *wsc1Δ* (MY15912) were transformed with a centromere-based plasmid containing Fus2p internally tagged with mCherry (a functional version of Fus2p, MR5821). Cells were exposed to pheromone for 1.5 h, fixed in 2% formaldehyde for 10 min and imaged. Cdc42p and Fus2 do not colocalize in WT or *wsc1Δ* shmoos, but do in *mid2Δ* shmoos. (D) Representative images of shmoos quantified in E; error bars represent SEM. *n* > 30. (F, G) CWI pathway sensor mutants do not affect Cdc42p localization in prezygotes. (F) Representative images of Cdc42p localization in WT (MY15747), *mid2Δ* (MY15910), or *wsc1Δ* (MY15912) cells mated to *fus1Δfus2Δ* (JY429) for 2.5 h, fixed with 2% formaldehyde, and imaged. Scale bars = 2 μm. (G) Quantification of GFP-Cdc42p fluorescence intensity in strains described in panel F. Fluorescence intensities are plotted as a ratio of the center to the average of the edges. Cdc42p formed a focus in WT, *mid2Δ*, and *wsc1Δ* prezygotes. *n* > 86 for all prezygotes.
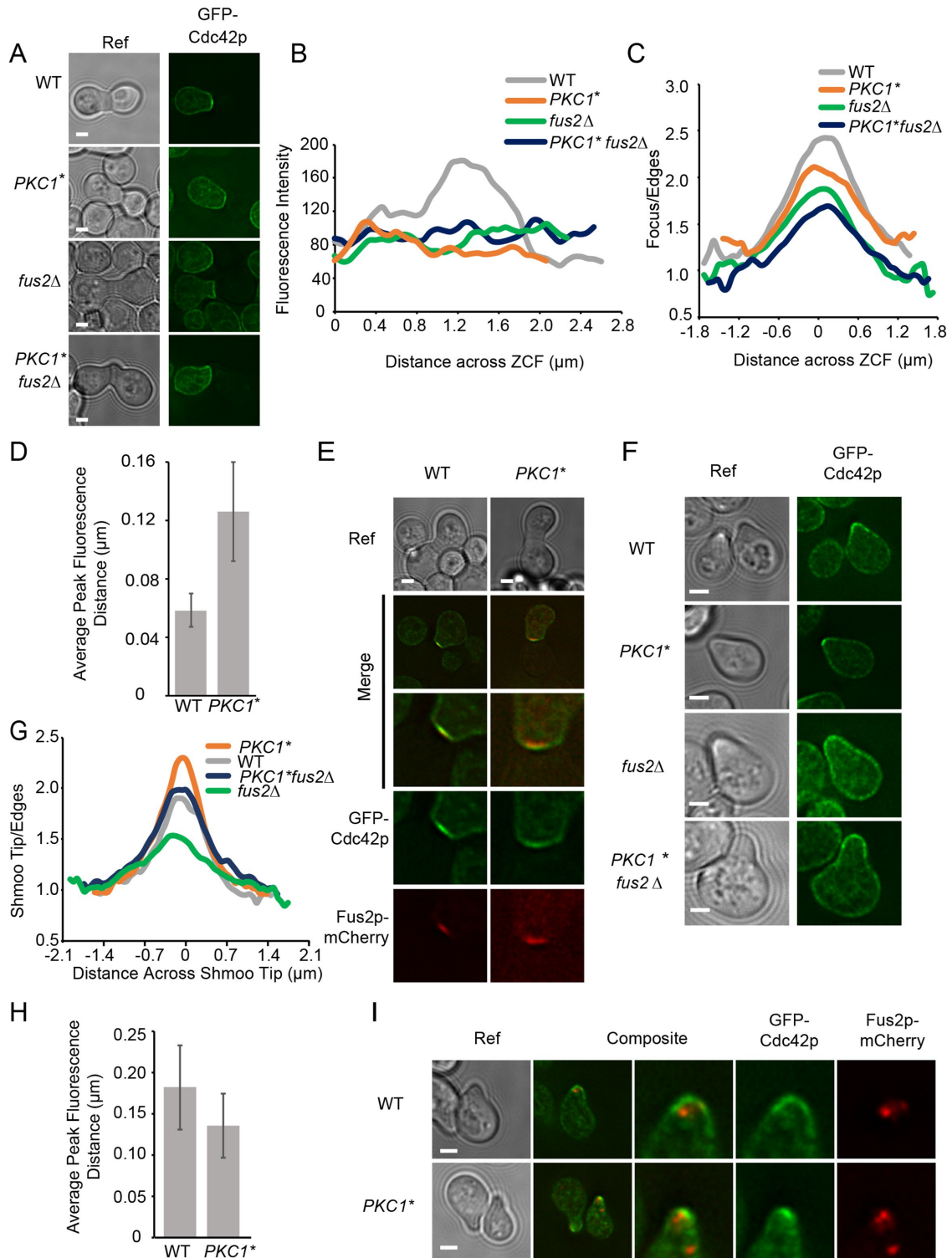
FIGURE 5: Pkc1p regulates Cdc42p in shmoos and prezygotes. (A, B, C) Cdc42p localization in *PKC1** prezygotes is partially Fus2p dependent. (A) Representative images of Cdc42p localization in WT (MY15747), *PKC1** (MY15902), *fus2Δ* (MY15717), and *PKC1*fus2Δ* (MY16005) mated to a *fus1Δ fus2Δ* (JY429) strain. (B) Fluorescence intensity measurements for each individual prezygote in panel A measured across the ZCF. (C) Combined fluorescence measurements across the ZCF, plotted as the ratio of intensity at each point relative to the edges; *n* > 91 for all prezygotes. (D, E) Cdc42p and Fus2p do not colocalize in *PKC1** prezygotes. Representative images and quantification of WT (MY15747) and *PKC1** (MY15902) cells transformed with a centromere-based plasmid containing Fus2p internally tagged with mCherry (MR5821) mated to a *fus1Δ fus2Δ* (JY429) strain; error bars denote SEM of three independent experiments. (F, G) *PKC1** increases Cdc42p localization to the shmoo tip. (F) Representative images and (G) quantification of Cdc42p focus at the shmoo tip. *PKC1** Cdc42-GFP (MY15902) has a Cdc42p focus at the shmoo tip compared with WT (MY15747). The *PKC1** Cdc42p focus is partially Fus2p dependent with decreased focus formation in *fus2Δ* (MY15717) and *PKC1* fus2Δ*

imply that Pkc1p regulates Cdc42p localization independent of recruitment by Fus2p, and that, in shmoos, Fus2p plays an indirect role in Cdc42p localization. Taken together with the decrease seen in wsc1Δ, we conclude that Cdc42p localization to the shmoo tip is driven in part by cues from cell wall remodeling, and this response is hyperactivated in PKC1* and different from what occurs in mid2Δ.

DISCUSSION

Negative regulation of cell fusion

Yeast cell fusion requires the concerted removal of the cell wall that separates the mating partners. Errors in the temporal and spatial regulation of cell wall removal would be catastrophic, implying the existence of multiple levels of regulation to insure the fidelity of mating. Previous work has largely focused on positive regulation of cell fusion, identifying multiple proteins required for cell wall removal. Several proteins (Fus1p, Spa2p, Bni1p) are thought to aid in the clustering of vesicles at the ZCF, whereas others are thought to facilitate their fusion with the plasma membrane and the subsequent release of hydrolases (Fus2p, Rvs161p, Cdc42p, and Kel1p; Trueheart et al., 1987; Trueheart and Fink, 1989; Gammie et al., 1998; Paterson et al., 2008; Ydenberg et al., 2012; Smith and Rose, 2016).

To mate, cells must sense when they are in contact with a mating partner to initiate cell wall removal. At the same time, cells monitor damage to their cell walls and respond by regulating proteins involved in repairing damage (Kono et al., 2012). The CWI pathway is activated in response to stresses on the cell wall during the polarized growth associated with budding and shmoo formation (Buehrer and Errede, 1997; Gray et al., 1997; Ketela et al., 1999). However, activation of the CWI pathway should interfere with the cell wall degradation that must occur for cell fusion to proceed. Consistent with this, PKC1*, encoding a hyperactive form of Pkc1p, causes a cell fusion defect (Philips and Herskowitz, 1997). It remained unclear whether the cell fusion defect results from increased cell wall repair or misregulation of the cell fusion machinery. To explore this question, we examined whether the mechanosensory transmembrane proteins, which surveil the cell wall and activate the CWI pathway, act as negative regulators of cell fusion (Dupres et al., 2009; Heinisch and Dufrene, 2010).

Wsc1p and Mid2p are the sole essential CWI pathway sensors; cells lacking both proteins cannot survive without osmotic support (Rajavel et al., 1999). Cells appear to grow normally when Wsc1p and Mid2p are the only sensors in the cell, implying that the remaining three sensors are not absolutely required (Supplemental Figure S1). In contrast, Mid2p has a unique function during mating, to regulate cell fusion. As a result, mid2Δ cells die in response to pheromone. In this work, we show that the pheromone-induced death of mid2Δ cells is caused by premature cell wall removal, specifically at the shmoo tip.

It was previously known that mid2Δ cells become sensitive to pheromone when grown in low calcium, but the mechanism remained unclear (Ketela et al., 1999; Rajavel et al., 1999). Mid2p contains a putative calcium binding domain (Ono et al., 1994) and was thought to be similar to Mid1p, a calcium transporter (Iida

et al., 1994). Both proteins were identified in a screen for mutants that were sensitive to pheromone in low calcium, but unlike mid1Δ, mid2Δ cells showed no defect in calcium uptake (Iida et al., 1990, 1994). Further confusing the issue, the mid2Δ pheromone-induced death is not suppressed by osmotic support, which suggested that death is not due to a cell wall defect (Rajavel et al., 1999), but instead reflects aberrant calcium signaling. Although the role of calcium remains unclear, suppression of mid2Δ pheromone-induced death by mutations affecting cell wall removal during mating (Figure 2A) supports the view that death is due to unregulated cell fusion.

Wsc1p localizes to sites of polarized growth during both shmoo formation and vegetative growth. In contrast, Mid2p becomes localized at the shmoo tip only during the pheromone response; otherwise, it is localized around the cell cortex (Delley and Hall, 1999; Ketela et al., 1999; Rajavel et al., 1999; Hutzler et al., 2008). If both sensors are located at the shmoo tip, why does wsc1Δ not cause pheromone-induced death? One possibility is that Wsc1p signaling is down-regulated during shmoo formation, so that Mid2p is the sole monitor of the cell wall in shmoos. Thus, a mid2Δ cell would have reduced activity of both major cell wall sensors, which would be a lethal combination. We think this is unlikely for two reasons. First, wsc1Δ decreased Cdc42p localization to the shmoo tip, suggesting that Wsc1p is indeed active. Second, in an assay for downstream activation of the CWI pathway, both wsc1Δ and mid2Δ cause reduced phosphorylation of Slt2p in response to pheromone (to 71 and 41% WT levels, respectively; Supplemental Figure S2B). An alternate possibility is that Mid2p has a unique function during mating, blocking Fus2p localization, possibly independent of its role in CWI signaling. Wsc1p and Mid2p occupy different microdomains within the plasma membrane, perhaps allowing for their differing functions (Kock et al., 2016). Regardless of the mechanism, Mid2p would prevent premature cell wall removal, and must be down-regulated in prezygotes to allow cell fusion.

Loss of either Wsc1p or Mid2p suppressed the fusion defect seen in fus1Δ × fus1Δ or fus2Δ × fus2Δ matings (Figure 2B), supporting the idea that the CWI pathway negatively regulates fusion and demonstrating that in prezygotes, both sensors are active. Suppression of fus1Δ and fus2Δ further suggests that cell fusion is mediated in part by the balance between cell wall removal and cell wall repair. Loss of either Fus1p or Fus2p would cause a reduced rate of cell wall removal, which can be easily counteracted by the CWI pathway. Reducing cell wall repair, in turn, by loss of a CWI sensor, would allow cell fusion to proceed by the remaining cell fusion machinery. However, some mating-enhanced cell wall removal is still required for fusion; loss of a CWI sensor is not sufficient to drive fusion when cells lack both Fus1p and Fus2p (Figure 2B).

It is not known at what level components of the CWI pathway regulate cell fusion. However, we think it unlikely that regulation entails activation of downstream signaling components. Under high osmolarity conditions, Slt2p phosphorylation was undetectable, yet suppression of fus2Δ was not greatly affected (Supplemental Figure S2, A and B). Therefore, the CWI pathway most likely regulates cell fusion upstream of Slt2p.

(MY16005); WT and fus2Δ data shown in Figure 4, B and C, as well. Fluorescence intensity was measured as described in Smith et al., 2017; fluorescence measured around the shmoo tip and plotted as a function of distance. Cells were incubated with pheromone for 1.5 h, fixed with 2% formaldehyde, and imaged. n > 86. (H, I) Cdc42p and Fus2p do not colocalize in PKC1* shmoos. Quantification and representative images of Cdc42p and Fus2p colocalization in PKC1* shmoos. WT (MY15747), PKC1* (MY15902), fus2Δ (MY15717), and PKC1* fus2Δ (MY16005) cells were exposed to pheromone for 1.5 h, fixed in 2% formaldehyde for 10 min, and imaged. n > 30. Scale bar = 2 μm.

Regulation of Cdc42p localization

Cdc42p is recruited to a focus at the ZCF specifically in prezygotes (Smith et al., 2017). In mid2Δ shmoos, a Cdc42p focus forms at the shmoo tip, dependent on and colocalizing with Fus2p (Figure 4). Given that Fus2p localizes to the ZCF independent of the interaction with Cdc42p (Smith et al., 2017), and that the proteins do not colocalize away from the ZCF, Mid2p may regulate the localization of Fus2p. Mid2p would thereby prevent the premature assembly of a Fus2p/Cdc42p complex which might initiate improper cell wall degradation.

In prezygotes, Cdc42p localization was found to be affected by curvature at the ZCF (Smith et al., 2017). When the ZCF is positively curved (projecting outward as in shmoos), Fus2p was localized, but formation of the Cdc42p focus was suppressed. One hypothesis to explain the sensitivity to curvature is that the amphiphysin-like Fus2p/Rvs161p heterodimer adopts a different conformation when it binds to flat membranes, conferring the ability to bind and recruit Cdc42p. An alternative possibility is that Mid2p, as a mechanosensor, may directly signal the changing curvature of the cell wall at the ZCF. In shmoos, and prezygotes with curved ZCFs, Mid2p would negatively regulate Fus2p association with the membrane and/or Cdc42p recruitment, preventing premature cell wall degradation. However, when cells come into contact and form a flat interface at the ZCF, negative regulation by Mid2p would be relieved, allowing for cell wall degradation and fusion to proceed. When mid2Δ cells found a mating partner and formed a prezygote before premature cell wall degradation, Cdc42p localization was WT, and fusion was unimpaired (Figure 4, F and G). It is likely, however, that both positive and negative regulation occur during cell fusion. Altering the curvature of the ZCF and hyperaction of PKC1 have additive effects (Philips and Herskowitz, 1997), suggesting that they may regulate cell fusion by independent pathways.

The role of Pkc1p in regulating Cdc42p localization is complex, apparently having different functions in shmoos and prezygotes. In shmoos, PKC1* caused the formation of a Cdc42p focus, superficially similar to the phenotype of mid2Δ. However, unlike mid2Δ, the Cdc42p focus did not colocalize with Fus2p (Figure 5, B–D), and PKC1* did not cause lysis in pheromone. Therefore, it is likely that PKC1*-driven localization reflects one of Cdc42p's several other functions, and not cell fusion–specific cell wall degradation. If so, it is confusing that PKC1*-driven Cdc42p localization is affected at all by Fus2p. One possibility is that, although Fus2p does not form a focus at the cortex, there is some Fus2p-dependent cell wall removal in shmoos. In support, β-1,3 glucan deposition at the tip of fus2Δ shmoos is increased, as assayed by aniline blue staining (Fitch et al., 2004). In addition, fus2Δ caused reduced Cdc42p localization to the shmoo tip in otherwise WT cells (Figure 4C). We speculate that Cdc42p localization in shmoos partially reflects cell wall assembly, as part of normal morphogenesis and the response to CWI signaling of cell wall degradation (Buehrer and Errede, 1997). In the presence of hyperactive Pkc1*p, some Fus2p-dependent cell wall degradation may lead to an exaggerated CWI response, observed as a large increase in Cdc42p localization.

In contrast, in prezygotes PKC1* caused decreased localization of Cdc42p to the ZCF. Decreased localization of Cdc42p, together with up-regulation of the CWI pathway, may explain the cell fusion defect caused by PKC1*. Interestingly, Fus2p localization to the ZCF occurred normally in PKC1* prezygotes, suggesting that Pkc1p may regulate the interaction between Fus2p and Cdc42p. In contrast, Mid2p appeared to regulate the localization of Fus2p. Thus, the different components of the CWI pathway may regulate cell

fusion by different mechanisms. It is interesting to note, as well, that during fission yeast mating, cells show a similar focus formation driving cell wall removal that is dependent on a MAPK cascade (Dudin et al., 2016). Fission yeast also show a dynamic patch of active Cdc42p at polarity sites; however, it was not possible to distinguish a role in fusion from roles in polarization and signaling (Merlini et al., 2018).

Understanding the role of cell wall degradation in yeast mating provides general insights into other cell fusion events. Even cells in higher eukaryotes must remove the intervening extracellular matrix to allow plasma membrane fusion with neighboring cells. Given the importance of such events and the detriment of improper fusion, it is likely that cells employ multiple levels of regulation to ensure that fusion proceeds safely. One general component of cell fusion regulation may be the application of a "brake" under conditions of cell surface stress or before successful engagement with a fusion partner.

MATERIALS AND METHODS

General yeast techniques

Yeast media, general methods, and transformations were performed as described previously (Amberg et al., 2005) with minor modifications. Strains and plasmids are listed in Supplemental Tables 1 and 2. All strains and plasmids are available upon request. Deletion strains were either created via PCR amplification of selective markers and homologous recombination at the locus of interest, or via crossing of various deletion strains followed by sporulation and tetrad dissection. All strains were grown at 30°C. For pheromone induction experiments, early exponential cells growing in selective media were treated for 90 min (unless otherwise specified) with synthetic α-factor (Department of Molecular Biology Syn/Seq Facility, Princeton University) added to a final concentration of 8 μg/ml.

For cells grown in low calcium media, yeast nitrogen base was made according to the formula from BD Sciences (San Jose, CA), but replacing all calcium salts with equivalent sodium salts.

Microscopy

All images were acquired at 23°C using a deconvolution microscopy system (DeltaVision; Applied Precision, LLC) equipped with an inverted microscope (TE200; Nikon) and a 100× objective with numerical aperture of 1.4. Deconvolution and image analysis were performed using Precision softWoRx and ImageJ (National Institutes of Health).

For imaging with propidium iodide, cells were prepared as described above and imaged after 3 h in pheromone. Cells were spun down and resuspended in phosphate-buffered saline (PBS), propidium iodide was added to a final concentration of 20 μm, and cells were incubated for 15 min at 23°C in the dark before imaging.

The Live/Dead Yeast Viability Kit (Invitrogen) was used according to protocol. Cells were prepared as above after 3 h in pheromone. A final concentration of 15 μm FUN-1 and 25 μm Calcofluor White were used before imaging.

Microscopic assays of FM4-64–stained mating mixtures and pheromone-induced cells were performed as described previously (Grote, 2008). Pheromone-induced cells were prepared as described and then resuspended in 1 ml of TAF buffer (20 mM Tris-HCl, 20 mM NaN$_3$, 20 mM NaF in water) and kept on ice. FM4-64 (Molecular Probes/Invitrogen) was added to cells to a final concentration of 4 μM and stained shmoos were imaged as above. For fusion assays, FM4-64 staining was used. An equal OD$_{600}$ (0.5) of each mating

type in log phase was mixed, concentrated on 25 mm 0.45 μm nitrocellulose filter disks (Millipore), and incubated on rich media plates for 2.5–3 h at 30°C.

For imaging of pheromone-induced cells with fluorescent proteins (Figures 4 and 5), cells were induced with pheromone in selective synthetic media for 90 min, fixed for 10 min with 2% formaldehyde at 30°C, washed in 1 X PBS, and then imaged in a smaller volume of PBS. A two-tailed, two-sample unequal *t* test of central peak values was used to determine significance.

For imaging of prezygotes containing fluorescent proteins, mating mixtures were prepared as described above, resuspended in synthetic media, fixed for 10 min with 2% formaldehyde at 30°C, and imaged as above. Quantification of fluorescence was performed using ImageJ software (Schindelin *et al.*, 2012, 2015). Fluorescence intensity was measured along a line contour corresponding to the ZCF or shmoo tip as described in Figure 1 of Smith *et al.* (2017). For prezygotes the contour extends the length of the ZCF; for shmoos the ends of the contour were defined by the middle of the inward curve of the shmoo neck. To account for cell to cell variation, fluorescence is expressed as the ratio of intensity divided by the average values for the 5 pixels (0.3 μm) at each end of the contour. The average end values represent regions in which Cdc42p did not appear to be concentrated. To combine data, contour measurements across the shmoo tip or ZCF were centered relative to one another to account for cell to cell variation in length. Two-tailed, heteroscedastic *t* tests were used to obtain *p* values for localization curves. Quantification of colocalization of Cdc42p and Fus2p was performed by quantifying fluorescence across a line perpendicular to the shmoo tip or ZCF using the ImageJ software. The peak was defined as the brightest pixel in the central focal plane for each cell. Error bars represent the standard error of the mean for all cells imaged. A two-tailed, two-sample unequal *t* test was used to determine significance.

Live imaging was performed by placing 0.04 OD_{600} of *mid2Δ* cells on a 2% agarose pad containing 8 μg/ml α-factor at 23°C. Images were taken at 1-min intervals using the DeltaVision system described above.

Electron microscopy

Cells were prepared for transmission electron microscopy as described in Gammie and Rose, 2002. Briefly, the workflow included a glutaraldehyde fixation, potassium permanganate staining, sodium periodate treatment, uranyl acetate staining, and embedding in LR White resin. Specifically, 40 ml of mid–log phase cells were grown in synthetic media without calcium, induced with 8 μg/ml α-factor at 30°C for 3 h, spun down, and fixed in 2% glutaraldehyde for 30 min at room temperature. Cells were stained with 4% potassium permanganate for 4 h at 4°C. Ultrathin sections (~80 nm) were placed on a nickel slotted grid (Formvar film, FF-2010-Ni; Electron Microscopy Sciences, Hatfield, PA) and imaged directly, without lead citrate staining.

REFERENCES
Abmayr SM, Pavlath GK (2012). Myoblast fusion: lessons from flies and mice. Development 139, 641–656.

Abmayr SM, Zhuang S, Geisbrecht ER (2008). Myoblast fusion in *Drosophila*. Methods Mol Biol 475, 75–97.

Adamo JE, Moskow JJ, Gladfelter AS, Viterbo D, Lew DJ, Brennwald PJ (2001). Yeast Cdc42 functions at a late step in exocytosis, specifically during polarized growth of the emerging bud. J Cell Biol 155, 581–592.

Alper S, Podbilewicz B (2008). Cell fusion in *Caenorhabditis elegans*. Methods Mol Biol 475, 53–74.

Amberg D, Burke D, Strathern J (2005). Methods in Yeast Genetics: A Cold Spring Harbor Laboratory Course Manual, Cold Spring Harbor, NY: Cold Spring Harbor Laboratory Press.

Baba M, Baba N, Ohsumi Y, Kanaya K, Osumi M (1989). Three-dimensional analysis of morphogenesis induced by mating pheromone alpha factor in *Saccharomyces cerevisiae*. J Cell Sci 94(Pt 2), 207–216.

Barale S, McCusker D, Arkowitz RA (2006). Cdc42p GDP/GTP cycling is necessary for efficient cell fusion during yeast mating. Mol Biol Cell 17, 2824–2838.

Bermejo C, Garcia R, Straede A, Rodriguez-Pena JM, Nombela C, Heinisch JJ, Arroyo J (2010). Characterization of sensor-specific stress response by transcriptional profiling of wsc1 and mid2 deletion strains and chimeric sensors in *Saccharomyces cerevisiae*. OMICS 14, 679–688.

Buehrer BM, Errede B (1997). Coordination of the mating and cell integrity mitogen-activated protein kinase pathways in *Saccharomyces cerevisiae*. Mol Cell Biol 17, 6517–6525.

de Bettignies G, Barthe C, Morel C, Peypouquet MF, Doignon F, Crouzet M (1999). RGD1 genetically interacts with MID2 and SLG1, encoding two putative sensors for cell integrity signalling in *Saccharomyces cerevisiae*. Yeast 15, 1719–1731.

Deere D, Shen J, Vesey G, Bell P, Bissinger P, Veal D (1998). Flow cytometry and cell sorting for yeast viability assessment and cell selection. Yeast 14, 147–160.

Delley PA, Hall MN (1999). Cell wall stress depolarizes cell growth via hyperactivation of RHO1. J Cell Biol 147, 163–174.

Di Gioia SA, Connors S, Matsunami N, Cannavino J, Rose MF, Gilette NM, Artoni P, de Macena Sobreira NL, Chan WM, Webb BD, *et al.* (2017). A defect in myoblast fusion underlies Carey-Fineman-Ziter syndrome. Nat Commun 8, 16077.

Drgonova J, Drgon T, Tanaka K, Kollar R, Chen GC, Ford RA, Chan CS, Takai Y, Cabib E (1996). Rho1p, a yeast protein at the interface between cell polarization and morphogenesis. Science 272, 277–279.

Dudin O, Merlini L, Martin SG (2016). Spatial focalization of pheromone/MAPK signaling triggers commitment to cell-cell fusion. Genes Dev 30, 2226–2239.

Dupres V, Alsteens D, Wilk S, Hansen B, Heinisch JJ, Dufrene YF (2009). The yeast Wsc1 cell surface sensor behaves like a nanospring in vivo. Nat Chem Biol 5, 857–862.

Dyer JM, Savage NS, Jin M, Zyla TR, Elston TC, Lew DJ (2013). Tracking shallow chemical gradients by actin-driven wandering of the polarization site. Curr Biol 23, 32–41.

Errede B, Cade RM, Yashar BM, Kamada Y, Levin DE, Irie K, Matsumoto K (1995). Dynamics and organization of MAP kinase signal pathways. Mol Reprod Dev 42, 477–485.

Fischer-Parton S, Parton RM, Hickey PC, Dijksterhuis J, Atkinson HA, Read ND (2000). Confocal microscopy of FM4–64 as a tool for analysing endocytosis and vesicle trafficking in living fungal hyphae. J Microsc 198, 246–259.

Fitch PG, Gammie AE, Lee DJ, de Candal VB, Rose MD (2004). Lrg1p is a Rho1 GTPase-activating protein required for efficient cell fusion in yeast. Genetics 168, 733–746.

Gammie AE, Brizzio V, Rose MD (1998). Distinct morphological phenotypes of cell fusion mutants. Mol Biol Cell 9, 1395–1410.

Gammie AE, Rose MD (2002). Assays of cell and nuclear fusion. Methods Enzymol 351, 477–498.

Gauster M, Moser G, Orendi K, Huppertz B (2009). Factors involved in regulating trophoblast fusion: potential role in the development of preeclampsia. Placenta 30 (suppl A), S49–S54.

Gray JV, Ogas JP, Kamada Y, Stone M, Levin DE, Herskowitz I (1997). A role for the Pkc1 MAP kinase pathway of *Saccharomyces cerevisiae* in bud emergence and identification of a putative upstream regulator. EMBO J 16, 4924–4937.

Grote E (2008). Cell fusion assays for yeast mating pairs. Methods Mol Biol 475, 165–196.

Heinisch JJ, Dufrene YF (2010). Is there anyone out there?—single-molecule atomic force microscopy meets yeast genetics to study sensor functions. Integr Biol (Camb) 2, 408–415.

Heinisch JJ, Rodicio R (2018). Protein kinase C in fungi—more than just cell wall integrity. FEMS Microbiol Rev 42. doi: 10.1093/femsre/fux051.

Huppertz B, Borges M (2008). Placenta trophoblast fusion. Methods Mol Biol 475, 135–147.

Hutzler F, Gerstl R, Lommel M, Strahl S (2008). Protein N-glycosylation determines functionality of the *Saccharomyces cerevisiae* cell wall integrity sensor Mid2p. Mol Microbiol 68, 1438–1449.

Iida H, Nakamura H, Ono T, Okumura MS, Anraku Y (1994). *MID1*, a novel *Saccharomyces cerevisiae* gene encoding a plasma membrane protein, is required for Ca^{2+} influx and mating. Mol Cell Biol 14, 8259–8271.

Iida H, Yagawa Y, Anraku Y (1990). Essential role for induced Ca^{2+} influx followed by $[Ca^{2+}]i$ rise in maintaining viability of yeast cells late in the mating pheromone response pathway. A study of $[Ca^{2+}]i$ in single *Saccharomyces cerevisiae* cells with imaging of fura-2. J Biol Chem 265, 13391–13399.

Ishii M, Saeki Y (2008). Osteoclast cell fusion: mechanisms and molecules. Mod Rheumatol 18, 220–227.

Jacoby JJ, Nilius SM, Heinisch JJ (1998). A screen for upstream components of the yeast protein kinase C signal transduction pathway identifies the product of the SLG1 gene. Mol Gen Genet 258, 148–155.

Jansen KM, Pavlath GK (2008). Molecular control of mammalian myoblast fusion. Methods Mol Biol 475, 115–133.

Jin H, Carlile C, Nolan S, Grote E (2004). Prm1 prevents contact-dependent lysis of yeast mating pairs. Eukaryot Cell 3, 1664–1673.

Johnson, DI (1999). Cdc42: an essential Rho-type GTPase controlling eukaryotic cell polarity. Microbiol Mol Biol Rev 63, 54–105.

Kamada Y, Qadota H, Python CP, Anraku Y, Ohya Y, Levin DE (1996). Activation of yeast protein kinase C by Rho1 GTPase. J Biol Chem 271, 9193–9196.

Ketela T, Green R, Bussey H (1999). *Saccharomyces cerevisiae* mid2p is a potential cell wall stress sensor and upstream activator of the PKC1-MPK1 cell integrity pathway. J Bacteriol 181, 3330–3340.

Kock C, Arlt H, Ungermann C, Heinisch JJ (2016). Yeast cell wall integrity sensors form specific plasma membrane microdomains important for signalling. Cell Microbiol 18, 1251–1267.

Kono K, Saeki Y, Yoshida S, Tanaka K, Pellman D (2012). Proteasomal degradation resolves competition between cell polarization and cellular wound healing. Cell 150, 151–164.

Kozminski KG, Chen AJ, Rodal AA, Drubin DG (2000). Functions and functional domains of the GTPase Cdc42p. Mol Biol Cell 11, 339–354.

Levin DE (2005). Cell wall integrity signaling in *Saccharomyces cerevisiae*. Microbiol Mol Biol Rev 69, 262–291.

Levin DE (2011). Regulation of cell wall biogenesis in *Saccharomyces cerevisiae*: the cell wall integrity signaling pathway. Genetics 189, 1145–1175.

Levin DE, Fields FO, Kunisawa R, Bishop JM, Thorner J (1990). A candidate protein kinase C gene, PKC1, is required for the *S. cerevisiae* cell cycle. Cell 62, 213–224.

Madden K, Snyder M (1998). Cell polarity and morphogenesis in budding yeast. Annu Rev Microbiol 52, 687–744.

Madhani HD (2007). From a to α: Yeast as a Model for Cellular Differentiation, Cold Spring Harbor, NY: Cold Spring Harbor Laboratory Press.

Mazur P, Baginsky W (1996). *In vitro* activity of 1,3-β-D-glucan synthase requires the GTP-binding protein Rho1. J Biol Chem 271, 14604–14609.

Merlini L, Dudin O, Martin SG (2013). Mate and fuse: how yeast cells do it. Open Biol 3, 130008.

Merlini L, Khalili B, Dudin O, Michon L, Vincenzetti V, Martin SG (2018). Inhibition of Ras activity coordinates cell fusion with cell-cell contact during yeast mating. J Cell Biol 217, 1467–1483.

Millard PJ, Roth BL, Thi HP, Yue ST, Haugland RP (1997). Development of the FUN-1 family of fluorescent probes for vacuole labeling and viability testing of yeasts. Appl Environ Microbiol 63, 2897–2905.

Mugnier S, Dell'Aquila ME, Pelaez J, Douet C, Ambruosi B, De Santis T, Lacalandra GM, Lebos C, Sizaret PY, Delaleu B, *et al.* (2009). New insights into the mechanisms of fertilization: comparison of the fertilization steps, composition, and structure of the zona pellucida between horses and pigs. Biol Reprod 81, 856–870.

Nern A, Arkowitz RA (1998). A GTP-exchange factor required for cell orientation. Nature 391, 195–198.

Nern A, Arkowitz RA (1999). A Cdc24p-Far1p-Gβγ protein complex required for yeast orientation during mating. J Cell Biol 144, 1187–1202.

Nonaka H, Tanaka K, Hirano H, Fujiwara T, Kohno H, Umikawa M, Mino A, Takai Y (1995). A downstream target of RHO1 small GTP-binding protein is PKC1, a homolog of protein kinase C, which leads to activation of the MAP kinase cascade in *Saccharomyces cerevisiae*. EMBO J 14, 5931–5938.

Ono T, Suzuki T, Anraku Y, Iida H (1994). The *MID2* gene encodes a putative integral membrane protein with a Ca^{2+}-binding domain and shows mating pheromone-stimulated expression in *Saccharomyces cerevisiae*. Gene 151, 203–208.

Ozaki K, Tanaka K, Imamura H, Hihara T, Kameyama T, Nonaka H, Hirano H, Matsuura Y, Takai Y (1996). Rom1p and Rom2p are GDP/GTP exchange proteins (GEPs) for the Rho1p small GTP binding protein in *Saccharomyces cerevisiae*. EMBO J 15, 2196–2207.

Passow H, Rothstein A, Loewenstein B (1959). An all-ornone response in the release of potassium by yeast cells with methylene blue and other basic redox dyes. J Gen Physiol 43, 97–107.

Paterson JM, Ydenberg CA, Rose MD (2008). Dynamic localization of yeast Fus2p to an expanding ring at the cell fusion junction during mating. J Cell Biol 181, 697–709.

Perez P, Rincon SA (2010). Rho GTPases: regulation of cell polarity and growth in yeasts. Biochem J 426, 243–253.

Philip B, Levin DE (2001). Wsc1 and Mid2 are cell surface sensors for cell wall integrity signaling that act through Rom2, a guanine nucleotide exchange factor for Rho1. Mol Cell Biol 21, 271–280.

Philips J, Herskowitz I (1997). Osmotic balance regulates cell fusion during mating in *Saccharomyces cerevisiae*. J Cell Biol 138, 961–974.

Qadota H, Python CP, Inoue SB, Arisawa M, Anraku Y, Zheng Y, Watanabe T, Levin DE, Ohya Y (1996). Identification of yeast Rho1p GTPase as a regulatory subunit of 1,3-β-glucan synthase. Science 272, 279–281.

Rajavel M, Philip B, Buehrer BM, Errede B, Levin DE (1999). Mid2 is a putative sensor for cell integrity signaling in *Saccharomyces cerevisiae*. Mol Cell Biol 19, 3969–3976.

Reinoso-Martin C, Schuller C, Schuetzer-Muehlbauer M, Kuchler K (2003). The yeast protein kinase C cell integrity pathway mediates tolerance to the antifungal drug caspofungin through activation of Slt2p mitogen-activated protein kinase signaling. Eukaryot Cell 2, 1200–1210.

Richman TJ, Sawyer MM, Johnson DI (1999). The Cdc42p GTPase is involved in a G2/M morphogenetic checkpoint regulating the apical-isotropic switch and nuclear division in yeast. J Biol Chem 274, 16861–16870.

Schindelin J, Arganda-Carreras I, Frise E, Kaynig V, Longair M, Pietzsch T, Preibisch S, Rueden C, Saalfeld S, Schmid B, *et al.* (2012). Fiji: an open-source platform for biological-image analysis. Nat Methods 9, 676–682.

Schindelin J, Rueden CT, Hiner MC, Eliceiri KW (2015). The ImageJ ecosystem: an open platform for biomedical image analysis. Mol Reprod Dev 82, 518–529.

Simon MN, De Virgilio C, Souza B, Pringle JR, Abo A, Reed SI (1995). Role for the Rho-family GTPase Cdc42 in yeast mating-pheromone signal pathway. Nature 376, 702–705.

Smith JA, Hall AE, Rose MD (2017). Membrane curvature directs the localization of Cdc42p to novel foci required for cell-cell fusion. J Cell Biol 216, 3971–3980.

Smith JA, Rose MD (2016). Kel1p mediates yeast cell fusion through a Fus2p- and Cdc42p-dependent mechanism. Genetics 202, 1421–1435.

Stein RA, Smith JA, Rose MD (2015). An amphiphysin-like domain in Fus2p is required for Rvs161p interaction and cortical localization. G3 (Bethesda) 6, 337–349.

Trueheart J, Boeke JD, Fink GR (1987). Two genes required for cell fusion during yeast conjugation: evidence for a pheromone-induced surface protein. Mol Cell Biol 7, 2316–2328.

Trueheart J, Fink GR (1989). The yeast cell fusion protein FUS1 is O-glycosylated and spans the plasma membrane. Proc Natl Acad Sci USA 86, 9916–9920.

Verna J, Lodder A, Lee K, Vagts A, Ballester R (1997). A family of genes required for maintenance of cell wall integrity and for the stress response in *Saccharomyces cerevisiae*. Proc Natl Acad Sci USA 94, 13804–13809.

Wassarman PM, Litscher ES (2008). Mammalian fertilization is dependent on multiple membrane fusion events. Methods Mol Biol 475, 99–113.

Yadav VR, Prasad S, Kannappan R, Ravindran J, Chaturvedi MM, Vaahtera L, Parkkinen J, Aggarwal BB (2010). Cyclodextrin-complexed curcumin exhibits anti-inflammatory and antiproliferative activities superior to those of curcumin through higher cellular uptake. Biochem Pharmacol 80, 1021–1032.

Ydenberg CA, Rose MD (2008). Yeast mating: a model system for studying cell and nuclear fusion. Methods Mol Biol 475, 3–20.

Ydenberg CA, Stein RA, Rose MD (2012). Cdc42p and Fus2p act together late in yeast cell fusion. Mol Biol Cell 23, 1208–1218.

Zhang NN, Dudgeon DD, Paliwal S, Levchenko A, Grote E, Cunningham KW (2006). Multiple signaling pathways regulate yeast cell death during the response to mating pheromones. Mol Biol Cell 17, 3409–3422.

Zhao ZS, Leung T, Manser E, Lim L (1995). Pheromone signalling in *Saccharomyces cerevisiae* requires the small GTP-binding protein Cdc42p and its activator CDC24. Mol Cell Biol 15, 5246–5257.